

Preparation and Characterization of Eco-friendly Carboxymethyl Cellulose Antimicrobial Nanocomposite Hydrogels

Sawsan Dacrory^{1*}, Hussein Abou-Yousef¹, Ragab E. Abou-Zeid¹, Samir Kamel¹, Mohamed S. Abdel-Aziz² and Mohamed Elbadry³

¹Cellulose and Paper Department, National Research Centre, 33 El Buhouth St., Dokki, Giza 12622, Egypt

²Microbial Chemistry Department, National Research Centre, 33 El Buhouth St., Dokki, Giza 12622, Egypt

³Department of Chemistry, Faculty of Science, Ain Shams University, Abbassia, Cairo 11566, Egypt

Received Month 25, 2017; Accepted December 2, 2017

ABSTRACT Carboxymethyl cellulose hydrogels were developed through crosslinking process using eco-friendly crosslinkers such as maleic, succinic, and citric acids. Carboxymethyl cellulose was prepared from the cellulosic fraction of olive industry residues. A series of hydrogels with varying crosslinker acid concentrations, reaction times, and reaction temperatures was produced to study the swelling capacities and gel fraction of the obtained hydrogels. Additional study pertains to the preparation of antimicrobial nanocomposite hydrogels through *in-situ* incorporation of the silver nanoparticles during the crosslinking reaction. Silver nanoparticles were prepared by reduction of AgNO₃ with leaves of *Ricinus communis*. The particle size of prepared silver nanoparticles was detected by transmission electron microscopy (TEM). Chemical structure and morphological characterizations of the prepared hydrogels were performed using Fourier transform infrared spectroscopy (FTIR), scanning electron microscopy (SEM), and energy-dispersive X-ray spectroscopy (EDX). Finally, the antimicrobial activity of the loaded silver hydrogels against Gram negative (G^{-ve}), Gram positive (G^{+ve}), and *Candida albicans* yeast was demonstrated.

KEYWORDS: Hydrogel, crosslinked carboxymethyl cellulose, silver nanoparticles, antibacterial activity

1 INTRODUCTION

Carboxymethyl cellulose (CMC) is considered as one of the most important cellulose derivatives, which has great importance in industry and everyday life. CMC is a linear, long-chain, water-soluble, and anionic polysaccharide derived from cellulose. Additionally, CMC is a white to cream colored as well as tasteless, odorless, and water-soluble polysaccharide with high molecular weight properties [1].

The value of CMC comes from its properties, such as nontoxicity biocompatibility and biodegradability, which make it suitable for widespread use in industrial and biomedical fields [2]. It has lots of applications in the textile, paper, detergent, pharmaceutical, food, and ceramic industries, among others. So, it is

produced in much higher amounts than any other cellulose derivative.

Polycarboxylic acids with multi-carboxyl groups, such as succinic, maleic, and citric acids, were chosen as solubilizing and crosslinking agents in the preparation of CMC-based hydrogel [3] for the following reasons: firstly, besides its multi-carboxylic structure, interaction can take place between the carboxyl groups of acids and the hydroxyl groups on CMC as an esterification reaction; this interaction would improve the water resistibility due to hydrophobic ester groups [4]. Secondly, the carboxyl groups of acid can form stronger hydrogen bonds with the hydroxyl groups of CMC chain. Furthermore, because of the multi-carboxyl structure, acid may serve as a crosslinking agent and, hence, it may improve the mechanical properties and water resistibility [5]. Thirdly, acid is rated as nutritionally harmless since it is a nontoxic metabolic product of the body [6].

Recently, the study and preparation of inorganic particles on the nanometer scale has been of great interest in both fundamental and applied research

*Corresponding author: sawsannrc2012@yahoo.com

DOI: 10.7569/JRM.2017.634190

[7]. It is well known that the physical and mechanical properties of nanoparticles are different from those of macroscopic material. Costly metal nanoparticles are utilized in solving the problems of water purification, catalysis and hydrogen storage. A broad range of applications have been created for metal nanoparticles in catalysis [8], electronics [9] sensors and high-density information storage [10], luminescence devices [11], photonics [12], pharmaceuticals, biotechnology and medicine. Nanoparticles are stabilized and grown in hydrogel networks due to available free-network spaces in the gel. Generally, the *in-situ* reduction of metal ions and stabilization of particles can be explained as (a) firstly, the metal ions are attached by functional groups of hydrogel networks and major amounts of them are diffused in the free-network spaces of hydrogels, (b) the reduction process takes place where some reducing agents are added for this purpose, (c) after that the formed particles are stabilized by the hydrogel network chains [13]. The formed nanoparticles in the gel effectively prevent the aggregation for longer periods and can be removed by water whenever they are required for usage. Moreover, these nanocomposite systems are highly appropriate for biomedical applications due to their good biocompatibility and biological molecules, cells, tissues, etc. Another advantage of this method is that the size and morphology of the nanoparticles can be controlled by altering their functionality and crosslinking points. Recently, many researchers have expended great effort to produce hydrogels containing silver nanoparticles (AgNPs), which are highly suitable for biomedical applications [14]. AgNPs have received much attention to control infections [15]. The antibacterial properties of AgNPs compared with bulk silver are attributed to high surface area and high fraction of surface atoms, which lead to penetration of more nanoparticles inside the bacteria and promote their efficacy in a sustained manner [7]. The main advantage of AgNPs is that even nanomolar concentrations are more effective than the micromolar concentrations of silver ions [16]. Also, AgNPs have a nontoxic effect on human cells [17]. Nanoparticles can be interpenetrated into the hydrogel matrix by a one-step process by mixing the nanoparticles with the preformed hydrogel during the gelation process, or in two steps by adding the nanoparticles during the swelling of the material [18, 19].

Previously, AgNPs were synthesized from plant leaf extracts. *Ricinus communis* leaf extract was used for the biosynthesis of AgNPs with antimicrobial activity against G-(+ve) bacterium *Bacillus fusiformis* and the G-(-ve) bacterium *Escherichia coli* [20]. Moreover, Mani *et al.* [21] used the extract of the green leaves of *Ricinus communis* for the green synthesis of AgNPs and these

biosynthesized nanoparticles could be used in both medical and technological applications. In addition, AgNPs were also biologically synthesized from leaf extract of the plant *Capparis spinosa* [22] and the produced nanoparticles exhibited excellent antimicrobial activity against G +ve and G -ve pathogenic bacteria such as *E. coli*, *Salmonella typhimurium*, *Staphylococcus aureus* and *Bacillus cereus*. *Ricinus communis* leaf extract was also used for the biosynthesis of AgNPs with antimicrobial activity against G +ve and G -ve bacteria [23].

In our previous work [24], we prepared AgNPs-loaded hydrogels by *in-situ* reduction of AgNO₃ through crosslinking of purchased CMC by polycarboxylic organic acids. In the current work, CMC is prepared from the cellulosic fraction of olive industry residues. Optimization of prepared CMC hydrogels is achieved via studying different preparation conditions like time, temperature and different polycarboxylic acids. Additionally, AgNPs are prepared by reduction of AgNO₃ with leaves of *Ricinus communis*. Finally, the antimicrobial activity of the loaded AgNPs hydrogels against G -ve, G +ve and *Candida albicans* yeast are demonstrated.

2 MATERIALS AND EXPERIMENTAL

2.1 Materials

Cellulose was extracted from olive oil by-product, succinic and citric acids and maleic anhydride were purchased from Riedel-de H en, *Ricinus communis* was grown and collected in the agricultural area around the canal bank area in Dekernes, Dakahlia governate, Egypt, and silver nitrate was purchased from Acros.

2.2 Experimental

2.2.1 Carboxymethylation

The synthesis of CMC was carried out based on the procedures of Heidrich and Ullmann with some modification. In brief, 2 g of cellulose in 53 ml of isopropanol was stirred vigorously while 10 ml of 40% aqueous sodium hydroxide solution was added during 20 min at room temperature. Stirring was continued for another 1 h at 40 °C, an equimolar amount of monochloroacetic acid (2.4 g dissolved in 5 mL organic solvent) was then added during 20 min. The mixture was allowed to react for 4 h at 30 °C. After carboxymethylation, the mixture was filtered, washed with methanol (70%) and neutralized with acetic acid. The product was collected, washed three times with 70% (w/w) aqueous ethanol and then dried at 45 °C in a vacuum oven [24].

2.2.1.1 Determination of Degree of Substitution

2.2.1.1.1 Purification of Carboxymethyl

Exactly 0.5 g of CMC was dissolved in 10 ml of water with stirring then 10 ml of 1 M hydrochloric acid was added and the mixture was agitated to dissolve completely. Five drops of phenolphthalein indicator were added to the mixture, and then 1 M sodium hydroxide was added dropwise with stirring until the appearance of red color. Ethanol (50 ml, 95%) was slowly added to the mixture with stirring and another 100 ml of 95% ethanol was added and the mixture was left to settle for 15 min. After the solution had settled the mixture was filtered by G₃-type glass cylinder and discarded. The precipitate was washed four times with 80% ethanol. The precipitate was washed again with 50 ml of 95% ethanol and dried in the oven at 105 °C for 4 h.

2.2.1.1.2 Degree of Substitution (DS)

The average values of the degree of substitution were determined by acidimetric titration. Exactly 0.2 g of CMC was weighed in a 250-ml flask, and then 50 ml distilled water was added with stirring for 10 min. The pH value of the solution was adjusted up to 8. Then the solution was titrated with 0.05 M H₂SO₄ until the pH value of solution decreased to 3.74. The degree of substitution was calculated based on the equations shown below [24]:

$$A = m_0/m \quad (1)$$

$$B = 2 \times M \times V/A \times m \quad (2)$$

$$DS = 0.132 \times B/1 - 0.08 \times B \quad (3)$$

where A is the purity of CMC, m₀ and m is the weight of purified carboxymethylated products after and before, M is the molarity of H₂SO₄ used, V is the volume of H₂SO₄ used to titrate sample, and B is the mmol/g of H₂SO₄ consumed per gram of carboxymethylated products.

2.2.2 Preparation of Hydrogel

Hydrogel preparation was carried out by using different polycarboxylic acids as crosslinkers. First, 1 g of CMC was dissolved in distilled water. Subsequently, the acid (maleic, succinic, or citric) was then added to the CMC solution in concentration ranging from 1.0 to 4.0% based on the weight of CMC. The mixture was then heated at different temperatures at different times under mild stirring. At the end of the reaction time, the sample was poured into a Petri dish and was placed in an oven at 45 °C [25].

2.2.3 Biosynthesis of Silver Nanoparticles from *Ricinus communis* Leaf

2.2.3.1 Preparation of Leaf Extract

The leaves of *Ricinus communis* (Family: Euphorbiaceae) were washed carefully using bi-distilled water to remove unnecessary materials. After removing water by using filter paper, 20 g of these leaves was finely cut and heated with 500 ml distilled water at 80 °C for 30 min and filtered through Whatman filter paper Grade 1 to obtain the extract. The produced extract was concentrated till dryness using a water evaporator at 80 °C. The produced extract exhibited a brownish color and a weight of 5 g. The extract (5 g) was redissolved in 5 ml of distilled water [26].

2.2.3.2 Synthesis of Silver Nanoparticles (AgNPs) Using Leaf Extracts

Silver nanoparticles (AgNPs) were synthesized by adding 100, 250, 750 and 1000 µl (separately) of *R. communis* leaf extract and 250 ml of 5 mM aqueous silver nitrate (AgNO₃) solution in an Erlenmeyer flask with a volume of 1000 ml. The flask was then kept in the dark (to diminish silver nitrate photooxidation) at room temperature. The produced AgNPs solution was purified by centrifugation at 13,000 rpm for 15 min followed by distribution of the pellet in distilled water [26].

2.2.4 Loading of AgNPs into Hydrogels

A definite amount of CMC was dissolved with continuous mechanical stirring until a homogeneous viscous mixture was obtained and then the crosslinker polycarboxylic acid was added. AgNPs solution (0.01, 0.009, 0.003, 0.002 Mol) was then added with continuous stirring at 80 °C for 30 min. The paste was dried in an oven at 45 °C.

2.2.5 Release of Silver from Hydrogels

Silver release was detected for the prepared AgNPs-loaded hydrogel of different crosslinking acids: maleic, citric, and succinic. For a typical run, 1.0 g of AgNPs-loaded hydrogel was immersed in 10 mL deionized water for different time intervals ranging from 1 to 24 h at ambient temperature. The immersed sample was separated from the deionized water, and a certain volume of deionized water including AgNPs was drawn for analysis by atomic absorption (Agilent Technologies 200 series AA), and the measurements were the average of four times. The mole percentage of AgNPs release was determined by calculating the mmole of AgNPs released (detected from the instrument), and the AgNPs loaded into the hydrogel

sample used for analysis (considering the stoichiometry of reduction reaction of silver cation).

$$\text{Mole of AgNPs release \%} = \frac{\text{(mmole of AgNPs release/mmole of loaded AgNPs in test sample)} \times 100}{\quad} \quad (4)$$

2.2.6 Antibacterial Activity

An agar plate method has been established to evaluate the antimicrobial activities of the prepared hydrogels [27]. Three different test microbes—*Staphylococcus aureus*, *Candida albicans*, and *Pseudomonas aeruginosa*—were selected to evaluate the antimicrobial activities as representatives of G +ve bacteria, G -ve bacteria, yeast and fungal groups. The bacterial and yeast test microbes were grown on a nutrient agar medium. On the other hand, the fungal test microbe was cultivated on Czapek-Dox medium. The culture of each test microbe was diluted by distilled water (sterilized) to 10⁷ to 10⁸ colony-forming units (CFU/ml), then 1 ml of each was used to inoculate a 1L-Erlenmeyer flask containing 250 ml of solidified agar media [28]. These media were put onto previously sterilized Petri dishes (10 cm diameter having 25 ml of solidified media). Hydrogel discs (10 mm Ø) were loaded and placed on the surface of the agar plates seeded with test microbes and incubated for 24 h at the appropriate temperature for each test organism. Antimicrobial activities were recorded as the diameter of the clear zones (including the gel film itself) that appeared around the gel films.

2.2.7 Characterization

2.2.7.1 Gel Fraction

Normally the hydrogel content of a given material is estimated by measuring its insoluble part in dried sample after immersion in deionized water for 24 h at room temperature. The obtained hydrogel was dried in a vacuum oven for 24 h and weighted (W_i), then it was soaked in distilled water for 24 h. The sample was then dried in a vacuum oven and weighted again (W_d). The gel fraction was then measured as follows [25]:

$$\text{Gel fraction \%} = \frac{(W_d/W_i) \times 100}{\quad} \quad (5)$$

2.2.7.2 Water Uptake (Swelling)

The progress of the water uptake (swelling) process was monitored gravimetrically as described by other workers [29]. In a typical swelling experiment, a pre-weighed piece of hydrogel (1 g) was immersed in an aqueous reservoir using distilled water and allowed to swell for a definite time period. The swollen piece was taken out at a predetermined time and pressed between two filter papers to remove excess water and weighed.

The water uptake and/or swelling percentage of hydrogel [30] can be determined as a function of time as follows:

$$\text{Water uptake (g/g)} = m_t - m_0 \quad (6)$$

$$\text{Swelling \%} = \frac{(m_t - m_0)}{m_0} \times 100 \quad (7)$$

where m_t is the weight of the swollen hydrogel sample at time t and m_0 is the weight of the dry hydrogel sample.

2.2.7.3 Fourier Transform Infrared Spectroscopy

The formed hydrogels were calibrated by using a Fourier transform infrared (FTIR) spectrometer (JASCO FT/IR-6100). To get the spectra, a pellet made from sample was ground with KBr. Transmission was measured at the wave number range of 800–4400 cm^{-1} .

2.2.7.4 Morphological Properties

The morphology of formed hydrogels (thin solid films successive by solvent) and CMC were observed using a scanning electron microscope (SEM) (Hitachi High Technologies America, Schaumburg, IL). Samples to be observed were mounted on conductive adhesive tape, coated with gold palladium, and observed under the SEM.

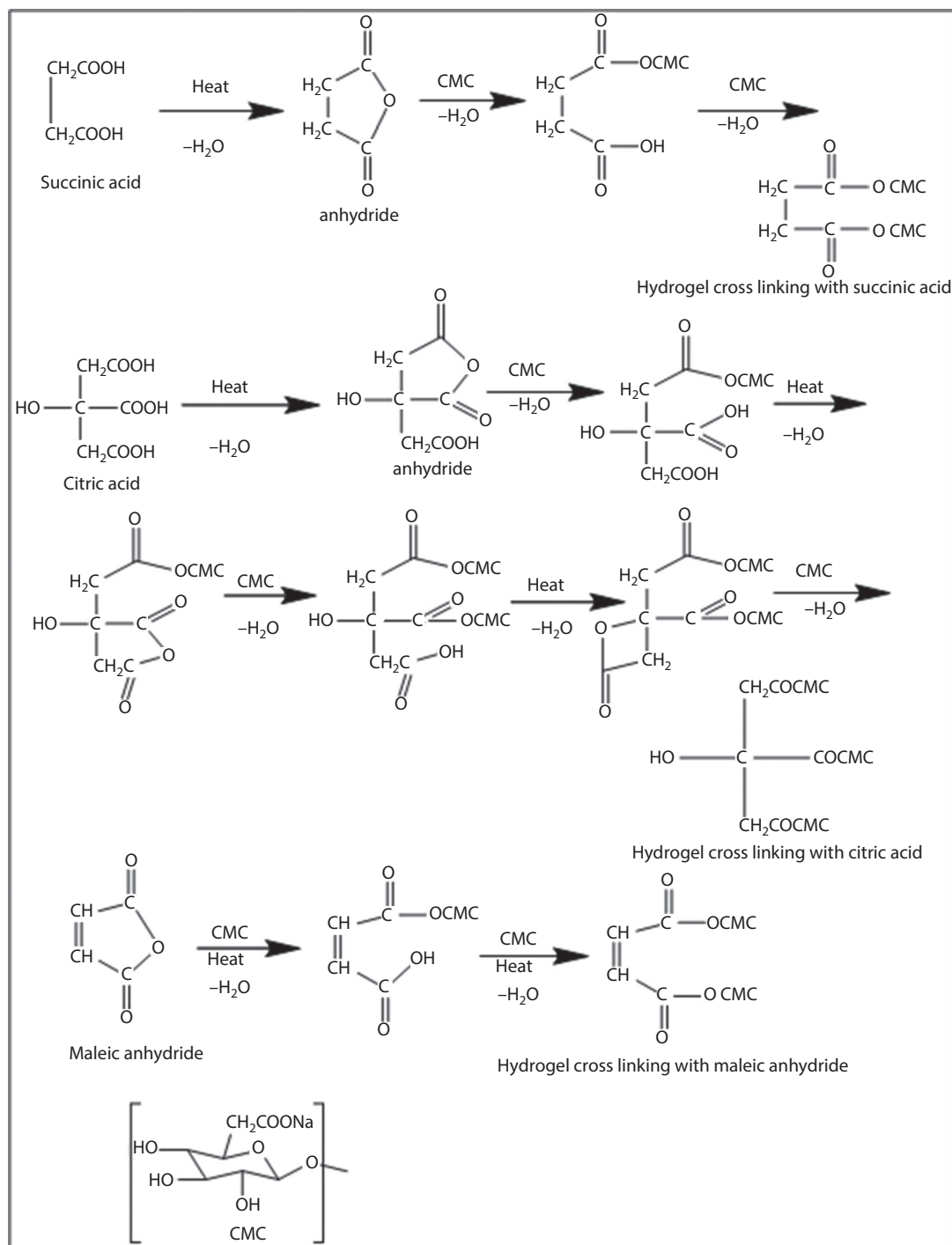
3 RESULTS AND DISCUSSION

3.1 Proposed Mechanism of Hydrogel Formation

In the formation of hydrogel due to the reaction of CMC with polycarboxylic acid the crosslinking occurs via esterification reaction between the hydroxyl group (OH) of CMC and carboxylic group (COOH) of acids as in Scheme 1. By heating, cyclic anhydride units were formed. This anhydride moiety of acids reacts with hydroxyl group in the main cellulosic chains to form an ester bond [25]. Also, dehydration between COOH groups and adjacent CMC molecules occurs to increase the strong hydrogen bonding during the thermal treatment [31].

3.2 Effect of Crosslinker

In this study, polycarboxylic acids, such as succinic acid, maleic anhydride, and citric acid, were used independently as crosslinker. As shown in Figures 1 and 2, increasing the polycarboxylic acid concentration led to an increase in the gel fraction and swelling of the prepared hydrogel until 2% acid concentration, then gel fraction and swelling decrease with further acid concentration. This is due to increasing



Scheme 1 Possible crosslinking reaction mechanism of polycarboxylic acids with CMC [25].

the acidity of the reaction medium while increasing the crosslinker, which leads to a change in the sodium salt form of CMC to an acidic form which is insoluble in the reaction medium; consequently, the chance of crosslinking points among CMC chains was decreased [25]. Accordingly, the optimum gel fraction (91, 79, and 78%) and swelling (525, 439, and 509%) were obtained

at 2% acid concentration for succinic, citric, and maleic acids respectively.

3.3 Effect of Reaction Temperature

Figures 3 and 4 show the effect of crosslinking temperature on gel fraction and swelling of the prepared

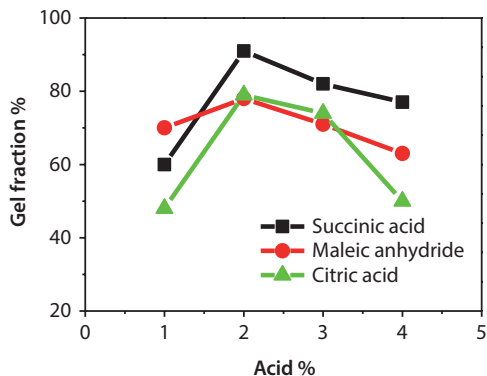


Figure 1 Effect of polycarboxylic acid concentration on gel fraction.

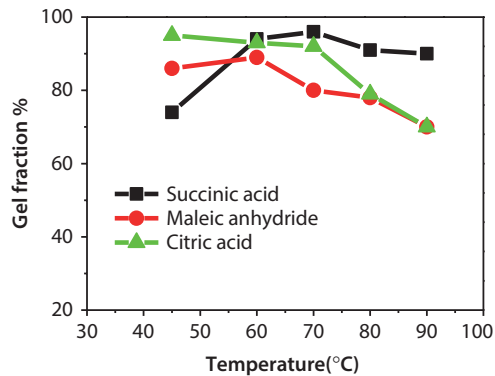


Figure 3 Effect of reaction temperature on gel fraction.

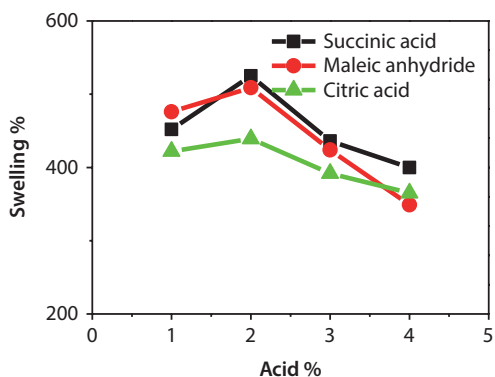


Figure 2 Effect of polycarboxylic acid concentration on swelling.

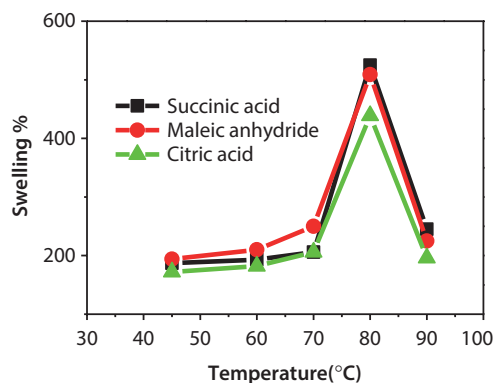


Figure 4 Effect of reaction temperature on swelling.

hydrogels. At 80 °C, the values of gel fractions % passed through maxima at 91, 79, and 78 where the optimum values of swelling % were 525, 439, and 509% for succinic, citric, and maleic anhydride respectively.

The explanation for the much higher swelling at 80 °C is based on the optimum temperature for forming the active intermediate compound necessary for the crosslinking process (anhydride species of polycarboxylic acids as illustrated in the proposed mechanism) behind the optimum crosslinking temperature. With the optimum crosslinking temperature of 80 °C, the rate of crosslinking reaction was vigorously enhanced, resulting in an increase of the crosslinking density of the hydrogel. Consequently, a reduction in the elasticity of the produced hydrogels emerged, leading to their decreased swelling.

3.4 Effect of Reaction Time

The effect of time on swelling and gel fraction is clear in Figures 5 and 6. The swelling and gel fraction have the highest value for citric acid and maleic anhydride

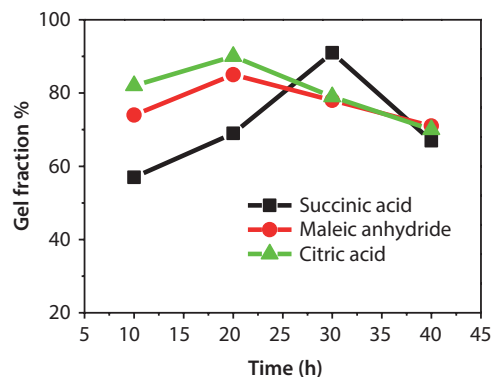


Figure 5 Effect of reaction time on gel fraction.

at 20 min, and the highest value for succinic acid is at 30 min, then starts to decrease due to dehydration between the COOH groups which form strong hydrogen bonding during the thermal treatment [32], which leads to decreased swelling and gel fraction.

The optimum gel fractions using succinic acid, citric acid, and maleic anhydride as crosslinkers are 91, 79, and 78, respectively, and the optimum swelling is 525, 509, and 439 for succinic acid, maleic anhydride, and

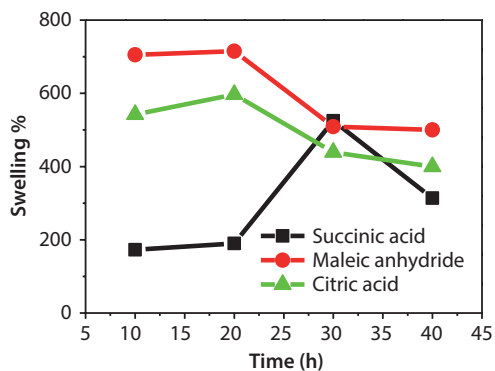


Figure 6 Effect of reaction time on swelling.

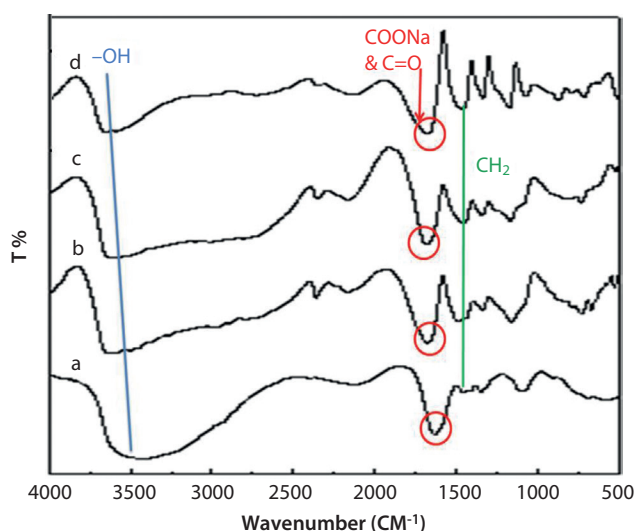


Figure 7 FTIR of (a) CMC, CMC crosslinked by (b) succinic acid (c) maleic anhydride, and (d) citric acid.

citric acid, respectively, with using 2% of acid at 80 °C for 20 min with citric acid and maleic anhydride and 30 min with succinic acid.

3.5 Characterization of Hydrogel

3.5.1 FTIR

Figure 7 shows the FTIR spectra of CMC and the CMC/hydrogels. In the CMC spectra the band at 3490 cm^{-1} is assigned to O-H stretching, and strong absorption band at 1626 cm^{-1} is due to the presence of COONa group. In the hydrogels' spectra the bands of O-H stretching are observed at a higher value of 3500–3546 cm^{-1} than in pure CMC due to hydrogen bond formation [31]. The band of C=O observed at 1672–1689 cm^{-1} shifted to a higher value than in CMC which referred to carbonyl ester formation; the bands at 1153, 1166 and 1178 cm^{-1} are due to ether linkage between CMC and

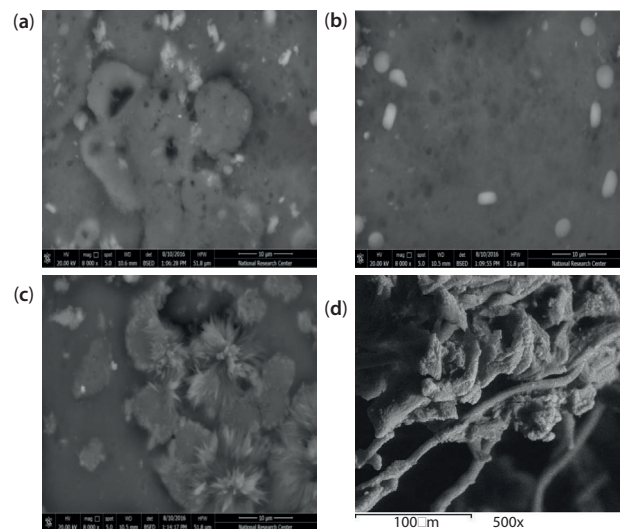


Figure 8 SEM of CMC/polycarboxylic hydrogel (a) succinic acid, (b) maleic anhydride, (c) citric acid, and (d) CMC.

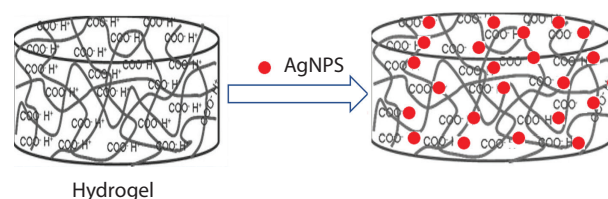


Figure 9 Loading of AgNPs onto hydrogel.

polycarboxylic acid; also, the band at 1400–1475 cm^{-1} is due to CH_2 bending vibrations which increased in hydrogel more than in pure CMC [25].

3.5.2 SEM

There is a difference in the surface morphology between pure CMC and CMC/gel. The SEM images of polycarboxylic hydrogels succinic acid, citric acid, and maleic anhydride appear in Figure 8; in CMC the surface appears in parallel chains crosslinked together, while in hydrogels these parallel chains disappeared and the surface became flat and contained some holes, which depended on network formation. In succinic and citric gels there are more holes on the surface than in the maleic gel surface.

3.6 Loading AgNPs onto Hydrogels

The concentrations of the prepared AgNPs were measured by an atomic absorption device and were 0.01, 0.009, 0.003, and 0.002 Mol/L.

The AgNPs were loaded onto hydrogels (Figure 9) through gelation and the color of gel turned from white to brown (Figure 10). The swelling and gel

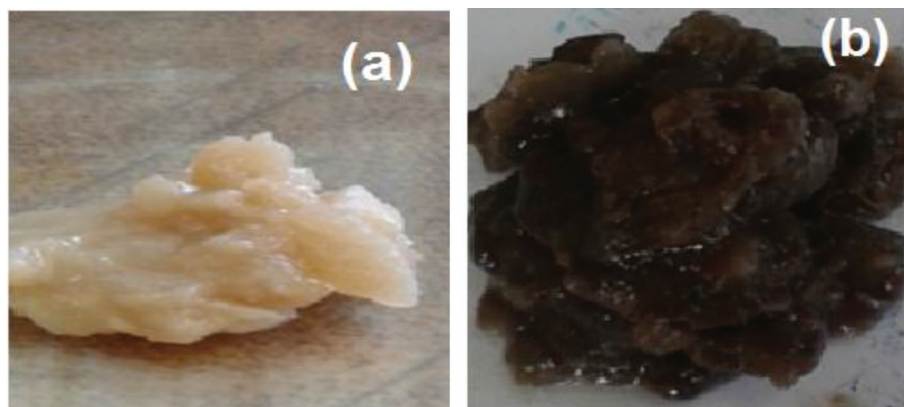


Figure 10 Photographs of hydrogels (a) without AgNPs, and (b) with AgNPs.

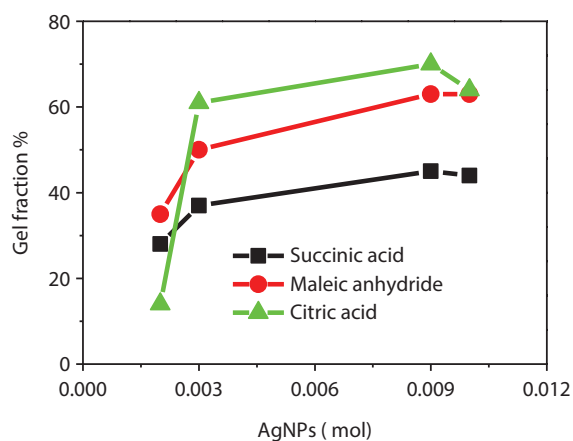


Figure 11 Effect of loaded AgNPs on gel fraction.

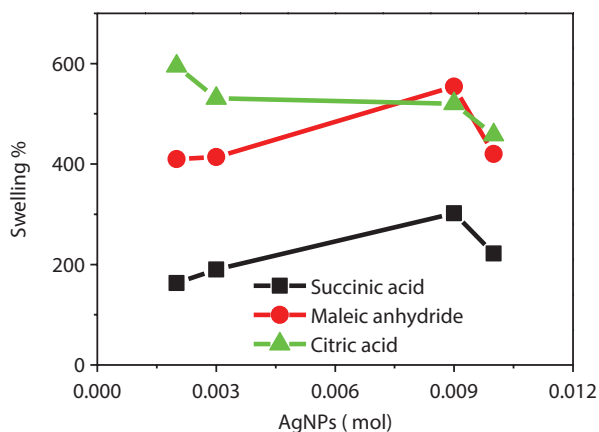


Figure 12 Effect of loaded AgNPs on swelling of hydrogel.

fraction of hydrogels with AgNPs (Figures 11 and 12) were increased until reaching the highest value at 0.009 mol and then started to decrease due to the presence of silver particles in the gel pores [25]. But in the case of citric acid, swelling decreased with

increasing AgNPs due to increasing bond formation and more crosslinking, which prevented the presence of AgNPs.

The effect of AgNPs on the swelling of hydrogel prepared with citric acid was explained according to the possibility of interaction between the AgNPs and the third carboxylic acid group which remained after the formation of anhydride species and completion of the first stage of crosslinking. This interaction may generate Ag cations, which can participate remarkably to perform further crosslinking among cellulose chains (via interaction with hydroxyl groups in the main chain). Consequently, increasing the crosslinking density of the prepared gel resulted in a decrease of swelling property.

3.6.1 Morphological Properties

The SEM images in Figure 13 show the distribution of AgNPs in hydrogels, which appear as white spherical particles on the surface of the hydrogels. From EDX analysis the highest loading of AgNPs was obtained in CMC/maleic gel and CMC/succinic gel, while the lowest loading was obtained by using citric acid as crosslinker. TEM was used to determine the particle size of the prepared AgNPs, which was between 29–54 nm, and particle size of prepared AgNPs inside the hydrogel, where the average size was between 14–35 nm, as shown in Figure 14.

3.6.2 Silver Release

Silver release from different crosslinking hydrogels is represented in Figure 15, which shows that the silver release in the beginning was rapid till 5 h, then started to slow down and became constant after 24 h. This may be attributed to the AgNPs presence in the holes of gel as a physical reaction so when it is put in water the AgNPs rapidly diffuse.

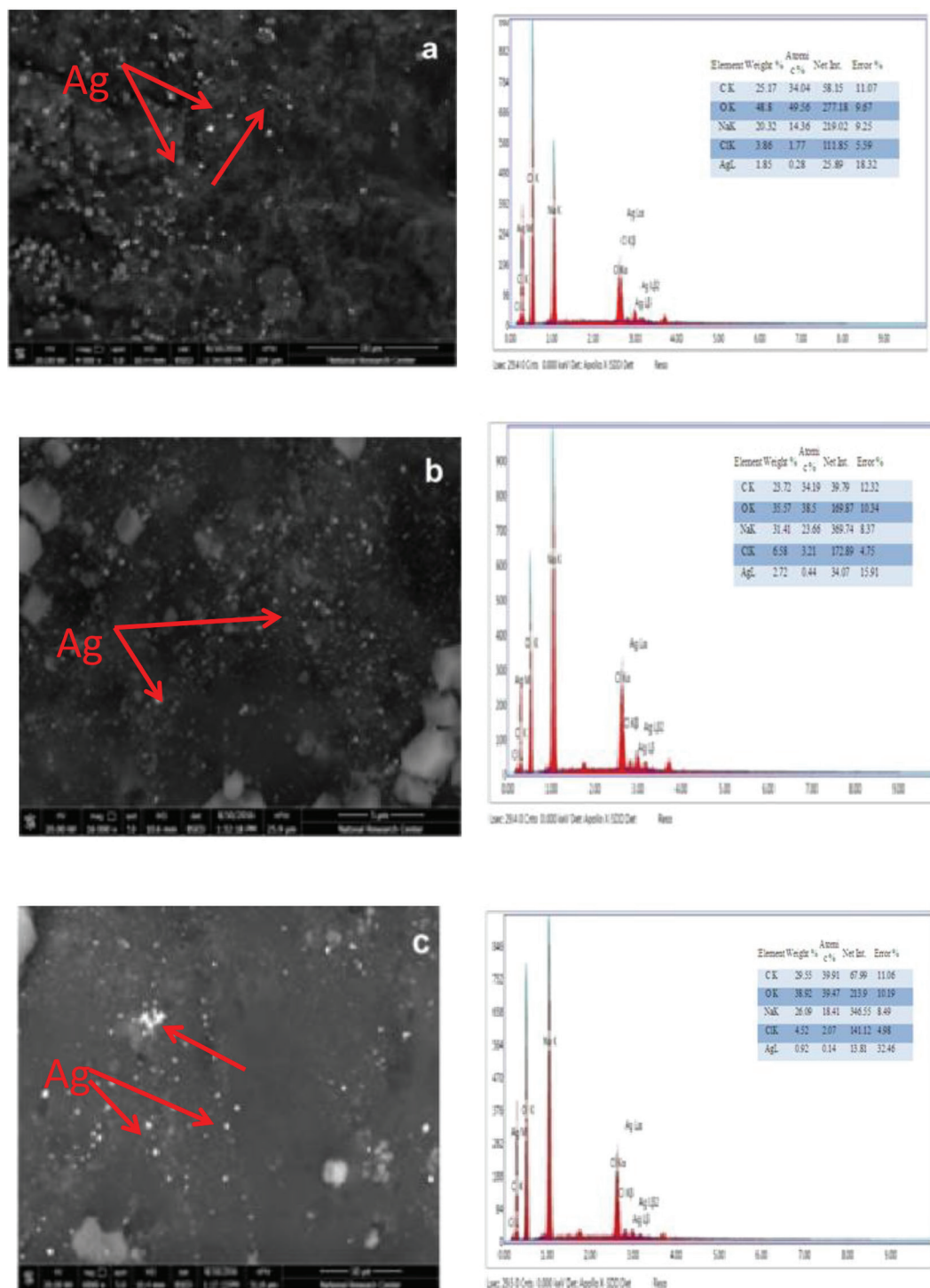


Figure 13 SEM and EDX of (a) CMC/succinic AgNPs, (b) CMC/maleic AgNPs, and (c) CMC/citric AgNPs.

3.6.3 Antibacterial Activity

Figure 16 shows the antibacterial activity of AgNPs-loaded hydrogels. The bioassay was carried out using G^{-ve} bacteria (*Pseudomonas aeruginosa*), G^{+ve} bacteria (*Staphylococcus aureus*), and *Candida albicans*. It appears

that the prepared AgNPs-loaded hydrogels have antibacterial properties, as evidenced by the appearance of an inhibition zone. By comparing the inhibition zones of different AgNPs-loaded hydrogels, the order is CMC/succinic gel is higher than CMC/maleic and CMC/citric.

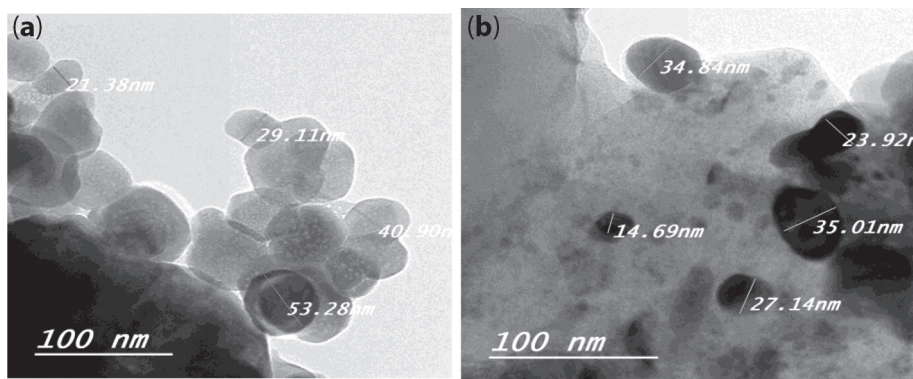


Figure 14 TEM of (a) AgNPs solution and (b) AgNPs in hydrogel.

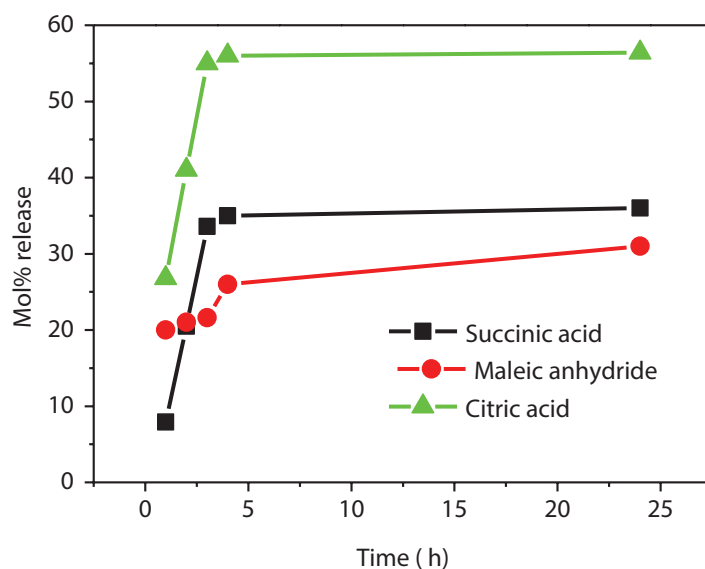


Figure 15 Release of silver from different hydrogels.

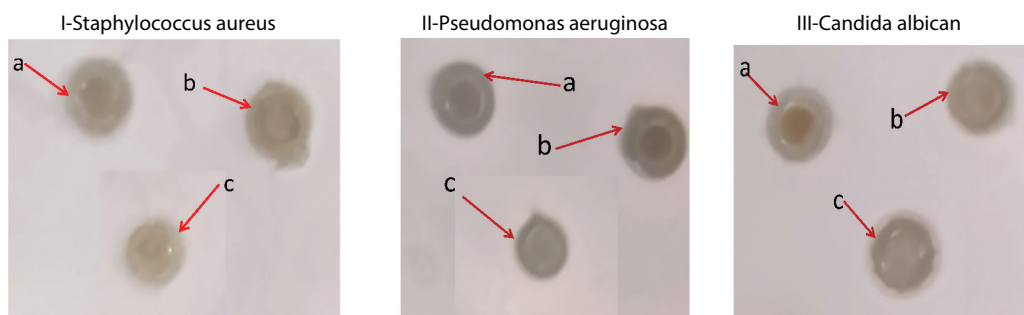


Figure 16 Antibacterial activities of AgNPs-loaded hydrogels with (a) succinic acid, (b) maleic anhydride, and (c) citric acid as crosslinker.

There are many mechanisms ascribed to the antimicrobial activity revealed by AgNPs, the best reliable mechanism is not fully understood; for example, the nanoparticles are established to act on diverse organisms in different ways and there are many theories on how the achievement of AgNPs on microbes causes the

microbicidal influence. AgNPs have the capability to attack the wall of bacterial cell and then penetrate it; in that way the AgNPs can cause structural changes in the cell membrane of the microbes and formation of “pits” on the cell surface, causing accumulation of AgNPs on the cell surface that lead to death of the microbes’ cell.

An alternative mechanism by which the cells die is the formation of free radicals by the AgNPs when they contact with microbial cells, and these free radicals have the aptitude to damage the cell membrane and make it porous, which can finally cause cell death [33,34].

4 CONCLUSION

A value-added product was prepared by carboxymethylation of the cellulosic fraction obtained from olive industry residues. Efficient antimicrobial hydrogels were prepared based on the crosslinking of AgNPs-loaded CMC. Polycarboxylic acids (citric, maleic, and succinic) were used as nontoxic crosslinking agents. An alternative method was performed to prepare AgNPs based on reduction of AgNO₃ with leaves of *Ricinus communis*, which produced lower particle size (50 nm) than that produced in the previous work (95 nm). Swelling properties of hydrogels were dependent on the crosslinker, where succinic acid showed the highest swellability. The loaded AgNPs enhanced the swellability of the hydrogels. Characterization of prepared hydrogels without and with loaded AgNPs was achieved by FTIR, SEM, TEM, and EDX methods. The loaded AgNP hydrogels showed antimicrobial activity towards *Staphylococcus aureus*, *Pseudomonas aeruginosa*, and *Candida albicans*, where inhibition zones were manifested.

REFERENCES

1. M.A. Bertuzzi, E.F. Castro, A.M. Vidaurre, and J.C. Gottifredi, Water vapor permeability of edible starch based films. *J. Food Eng.* **80**, 972–978 (2007).
2. C. Chang, L. Zhang, J. Zhou, L. Zhang, and J.F. Kennedy, Structure and properties of hydrogels prepared from cellulose in NaOH/urea aqueous solutions. *J. Carbohydr. Polym.* **82**, 122–127 (2010).
3. H. Chen, K.H. Hsieh, C.T. Tsao, C.H. Chang, Y.D. Li, M.F. Wu, C. P. Lin, J. L. Han, S. H. Chen, and K. H. Hsieh, Development of chitosan/dicarboxylic acid hydrogels as wound dressing materials. *J. Bioact. Compat. Polym.* **26**, 519–536 (2011).
4. E. Borredon, D. Bikiaris, J. Prinos, and C. Panayiotou, Properties of fatty-acid esters of starch and their blends with LDPE. *J. Appl. Polym. Sci.* **65**, 705–721 (1997).
5. R. Shi, Z.Z. Zhang, Q.Y. Liu, Y.M. Han, L.Q. Zhang, and D.F. Chen, Characterization of citric acid/glycerol coplasticized thermoplastic starch prepared by melt blending. *Carbohydr. Polym.* **69**, 748–755 (2007).
6. J. Yang, A. Webb, and G. Ameer, Novel citric acid-based biodegradable elastomers for tissue engineering. *Adv. Mater.* **16**, 511–516 (2004).
7. S.K. Bajpai, Y.M. Mohan, M. Bajpai, R. Tankhiwale, and V. Thomas, Synthesis of polymer stabilized silver and gold nanostructures. *J. Nanosci. Nanotechnol.* **7**, 2994–3010 (2007).
8. A. Biffis, N. Orlandi, and B. Corain, Microgel-stabilized metal nanoclusters: Size control by microgel nanomorphology. *J. Adv. Mater.* **15**, 1551–1555 (2003).
9. A. Kiesow, J.E. Morris, C. Radehaus, and A. Heilmann, Switching behavior of plasma polymer films containing silver nanoparticles. *J. Appl. Phys.* **94**, 6988–6990 (2003).
10. C.A. Ross, Patterned magnetic recording media. *Annu. Rev. Mater. Res.* **31**, 203–235 (2001).
11. V.L. Colvin, M.C. Schlamp, and A.P. Alivisatos, Light emitting-diodes made from cadmium selenide nanocrystals and a semiconducting polymer. *Nature* **370**, 354–357 (1994).
12. S. Xu, J. Zhang, C. Paquet, Y. Lin, and E. Kumacheva, From hybrid microgels to photonic crystals. *Adv. Funct. Mater.* **13**, 468–472 (2003).
13. C. Wang, N.T. Flynn, and R. Langer, Controlled structure and properties of thermoresponsive nanoparticle hydrogel composites. *Adv. Mater.* **16**, 1074–1079 (2004).
14. V. Thomas, M. Namdeo, Y. Mohan, S.K. Bajpai, and M. Bajpai, Review on polymer hydrogel and microgel metal nanocomposites: A facile nanotechnological approach. *J. Macromol. Sci. Part A. Pure Appl. Chem.* **45**, 107–119 (2008).
15. M. Rai, A. Yadav, and A. Gade, Silver nanoparticles as a new generation of antimicrobials. *Biotechnol. Adv.* **27**, 76–83 (2009).
16. H. Kong and J. Jang, Antibacterial properties of novel poly (methyl methacrylate) nanofiber containing silver nanoparticles. *Langmuir* **24**, 2051–2056 (2008).
17. K. Vimala, K.M. Mohan, K.S. Sivudu, K. Varaprasad, S. Ravindra, N.N. Reddy, Y. Padma, B. Sreedhar, and K. MohanaRaju, Fabrication of porous chitosan films impregnated with silver nanoparticles. A facile approach for superior antibacterial application. *Colloids Surf. B. Biointerfaces* **76**, 248–258 (2010).
18. L.M. Hamming, R. Qiao, P.B. Messersmith, and L.C. Brinson, Effects of dispersion and interfacial modification on the macroscale properties of TiO₂ polymer matrix nanocomposites. *Compos. Sci. Technol.* **69**, 1880–1886 (2009).
19. K. Haraguchi, R. Farnsworth, A. Ohbayshi, and T. Takehisa, Compositional effects on mechanical properties of nanocomposite hydrogels composed of poly(N,N-dimethylacrylamide) and clay. *Macromolecules* **36**, 5732–5741 (2003).
20. A. Singh, S. Mittal, R. Shrivastav, S. Dass, and J.N. Srivastava, Biosynthesis of silver nanoparticles using *Ricinus communis* L. leaf extract and its antibacterial activity. *Dig. J. Nanomat. Biostruct.* **7**(3), 1157–1163 (2012).
21. U. Mani, S. Dhanasingh, R. Arunachalam, E. Paul, P. Shanmugam, C. Rose, and A.B. Mandal, Simple and green method for the synthesis of silver nanoparticles using *Ricinus communis* leaf extract. *Prog. Nanotechnol. Nanomater.* **2**(1), 21–25 (2013).
22. F. Benakashani, A.R. Allafchian, and A.A.H. Jalali, Biosynthesis of silver nanoparticles using *Capparis spinosa* L. leaf extract and their antibacterial activity. *Karbala Int. J. Mod. Sci.* **2**, 251–258 (2016).
23. S. Ojha, A. Sett, and U. Bora, Green synthesis of silver nanoparticles by *Ricinus communis* var. *carmencita*

- leaf extract and its antibacterial study. *Adv. Nat. Sci.: Nanosci. Nanotechnol.* **8**, 035009 (2017).
24. S. Dacrory, H. Abou-Yousef, S. Kamel, R.E. Abou-Zeid, M.S. Abdel-Aziz, M. Elbadry, Utilization and characterizations of olive oil industry by-product. *WASET Int. J. Environ. Chem. Ecol. Geol. Geophys. Eng.* **10** (2016).
 25. A. Hussein and K. Samir, High efficiency antimicrobial cellulose-based nanocomposite hydrogels. *J. Appl. Polym. Sci.* **132**, 42327 (2015).
 26. N. Shanmugam, P. Rajkamal, S. Cholan, N. Kannadasan, K. Sathishkumar, G. Viruthagiri, and A. Sundaramanickam, Biosynthesis of silver nanoparticles from the marine seaweed *Sargassum wightii* and their antibacterial activity against some human pathogens. *Appl. Nanosci.* **4**, 13204–13271(2013).
 27. M.S. Abdel-Aziz, K.S. Abou-El-Sherbini, E.M.A. Hamzawy, M.H.A. Amr, and S. El-Dafrawy, Green synthesis of silver nanoparticles by *Macrococcus bovicus* and its immobilization onto montmorillonite clay for antimicrobial functionality. *Appl. Biochem. Biotechnol.* **176**, 2225–2241 (2015).
 28. A.M. Youssef, M.S. Abdel-Aziz, and S.M. El-Sayed, Chitosan nanocomposite films based on Ag-NP and Au-NP biosynthesis by *Bacillus subtilis* as packaging materials. *Int. J. Biol. Macromol.* **69**, 185-191 (2014).
 29. L.F. Gudeman, and N.A. Peppas, Preparation and characterization of pH-sensitive, interpenetrating networks of poly (vinyl alcohol) and poly (acrylic acid). *J. Appl. Polym. Sci.* **55**, 919-928 (1995).
 30. A. Kostic, B. Adnadjevic, A. Bopovic, and J. Jovanovic, Comparison of the swelling kinetics of a partially neutralized poly (acrylic acid) hydrogel in distilled water and physiological solution. *J. Serb. Chem. Soc.* **72**, 1139-1153 (2007).
 31. H. Ali, H. Mohamed, M.M. Abd El-Hady, and S. Sharaf, Development of CMC hydrogels loaded with silver nano-particles for medical applications. *Carbohydr. Polym.* **92**, 407–413 (2013).
 32. A. Taubert and G. Wegner, Formation of uniform and monodisperse zincite crystals in the presence of soluble starch. *J. Mater. Chem.* **12**(4), 805–807 (2002).
 33. M. Sadeghi, F. Soleimani, and M. Yarahmadi, Chemical modification of carboxymethyl cellulose via graft copolymerization and determination of the grafting parameters. *Orient. J. Chem.* **27**(3), 967–972 (2011).
 34. A.M. Youssef, S.A. Mohamed, M.S. Abdel-Aziz, M.E. Abdel-Aziz, G. Turky, and S. Kamel, Biological studies and electrical conductivity of paper sheet based on PANI/PS/Ag-NPs nanocomposite. *Carbohydr. Polym.* **147**, 333–343 (2016).